



ORIGINAL PAPERS

Dephosphorylated hypoxia-inducible factor 1 α as a mediator of p53-dependent apoptosis during hypoxia

Hiroyuki Suzuki¹, Akihiro Tomida¹ and Takashi Tsuruo^{*1,2}

¹Institute of Molecular and Cellular Biosciences, University of Tokyo, 1-1-1, Yayoi, Bunkyo-ku, Tokyo 113-0032, Japan; ²Cancer Chemotherapy Center, Japanese Foundation for Cancer Research, 1-37-1, Kami-Ikebukuro, Toshima-ku, Tokyo 170-0012, Japan

Under hypoxia, HIF-1 α binds to aryl hydrocarbon receptor nuclear translocator (ARNT, also called HIF-1 β) to activate expression of genes important for cell survival. Alternatively, HIF-1 α can bind to the tumor suppressor p53 and promote p53-dependent apoptosis. Here we show that the opposite functions of HIF-1 α are distinguished by its phosphorylation status. Two distinguishable forms of HIF-1 α , phosphorylated and dephosphorylated, were induced during hypoxia-induced apoptosis. The phosphorylated HIF-1 α was the major form that bound to ARNT. Ectopically expressed ARNT was consistently able to enhance HIF-1 α phosphorylation in a binding-dependent manner. In contrast, the dephosphorylated HIF-1 α was the major form that bound to p53. Depletion of the dephosphorylated HIF-1 α , by using the Hsp90 inhibitor geldanamycin A that had little effect on the phosphorylated HIF-1 α expression, suppressed p53 induction and subsequent apoptosis. Depletion of dephosphorylated HIF-1 α also prevented hypoxia-induced nuclear accumulation of HDM2, a negative regulator of p53. Our results indicate that the functions of HIF-1 α varied with its phosphorylation status and that dephosphorylated HIF-1 α mediated apoptosis by binding to and stabilizing p53. *Oncogene* (2001) 20, 5779–5788.

Keywords: apoptosis; HIF-1 α ; hypoxia; p53; phosphorylation

Introduction

HIF-1, the heterodimer of HIF-1 α and ARNT (HIF-1 β), is a basic helix–loop–helix (bHLH) / PAS (Per-ARNT-Sim) transcription factor that plays an essential role in O₂ homeostasis. To activate transcription of target genes, HIF-1 α dimerizes with ARNT and binds to consensus sequence 5'-RCGTG-3' within hypoxia-responsive elements (HRE). The target genes, such as vascular endothelial growth factor (VEGF), erythro-

poietin and various glycolytic enzymes, are involved in angiogenesis, erythropoiesis, energy metabolism and cell viability (for review see Semenza, 2000). Under normoxic conditions, HIF-1 α is ubiquitinated and subjected to degradation by proteasome (Salceda and Caro, 1997). Hypoxia prevents the ubiquitination of HIF-1 α , resulting in induction of HIF-1 α protein (Kallio *et al.*, 1999). Recent studies indicate that subsequent phosphorylation of HIF-1 α enhances the transcriptional activity of HIF-1 (Richard *et al.*, 1999). On the other hand, ARNT is constitutively expressed in the nucleus and acts as a common subunit of multiple bHLH-PAS family proteins (Crews, 1998). Thus, the hypoxic induction and modification of HIF-1 α determine the HIF-1 transcription activity for adapting to hypoxia.

Apoptosis is an evolutionarily conserved cell death mechanism that is activated by various stimuli. Hypoxia is also known to induce apoptosis that depends on the tumor suppressor p53 (Graeber *et al.*, 1996). Following stabilization as a result of apoptotic stimuli, p53 activates expression of various genes that are involved in apoptosis and growth arrest (Giaccia and Kastan, 1998; Vogelstein *et al.*, 2000). One of the most characterized pro-apoptotic genes inducible by p53 is Bax, a member of Bcl-2 family proteins, which translocates to mitochondria and releases cytochrome *c* to cytosol (Green and Reed, 1998). The Bax translocation to mitochondria is a critical step in p53-induced apoptosis (Deng and Wu, 2000). In cytosol, cytochrome *c* interacts with Apaf-1 to activate caspase-9 that, in turn, activates downstream caspases, such as caspase-3. The activated caspases cleave many substrates, stimulate the apoptotic cascade, and induce the morphological features of apoptosis (Nicholson, 1999).

Paradoxically, HIF-1 α is also involved in the hypoxia-induced apoptosis. HIF-1 α -deficient ES cells, which have impaired angiogenic potential, exhibit resistance to hypoxia due to impaired expression of p53 (Carmeliet *et al.*, 1998). In cultured cortical neurons, HIF-1 α promotes p53-dependent apoptosis (Halterman *et al.*, 1999). HIF-1 α binds to p53, and the complex formation likely plays an important role in the hypoxia-induced stabilization of p53 (An *et al.*, 1998). Thus, HIF-1 α has dual functions in response to hypoxia. One is for cell survival through binding to ARNT and the other is for cell death through binding to p53. However, it is not known how these opposite

*Correspondence: T Tsuruo, Institute of Molecular and Cellular Biosciences, University of Tokyo, 1-1-1, Yayoi, Bunkyo-ku, Tokyo 113-0032, Japan; E-mail: tsuruo@iam.u-tokyo.ac.jp
Received 9 March 2001; revised 13 June 2001; accepted 18 June 2001

functions of HIF-1 α are regulated under hypoxic conditions.

In this study, we present evidence that the dual functions of HIF-1 α are distinguished by its phosphorylation status. Indeed, both phosphorylated and dephosphorylated HIF-1 α were induced during hypoxia-induced apoptosis. We found that phosphorylated and dephosphorylated HIF-1 α form complexes with ARNT and p53, respectively. Moreover, we showed that inhibition of the emergence of dephosphorylated HIF-1 α suppressed apoptosis induced by p53. Our findings demonstrated that phosphorylation status of HIF-1 α was important for the regulation of cell survival and death under hypoxia.

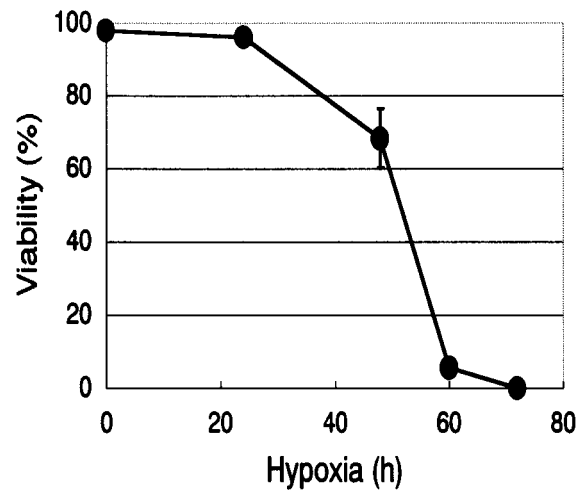
Results

Alteration in HIF-1 expression during hypoxia-induced apoptosis

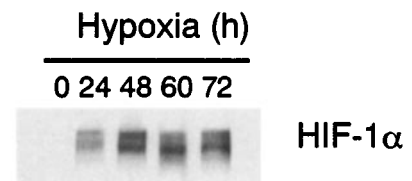
Exposure of human breast carcinoma MCF-7 cells to hypoxia for more than 48 h induced cell death (Figure 1a). The prolonged hypoxia caused nuclear condensation and loss of mitochondrial transmembrane potential, which are the features of apoptosis (data not shown). The same hypoxia treatment led to induction of HIF-1 α protein. Two major bands of HIF-1 α were detected by immunoblot analysis (Figure 1b). The slower migrated band was significantly reduced after 48 h; the faster was increased when hypoxia treatment was prolonged. The induction of faster migrated HIF-1 α correlated with induction of p53 (Figure 2b and below). To clarify the biochemical basis of the two major species of HIF-1 α , we treated immunoprecipitated HIF-1 α with λ phosphatase. Figure 1c shows that the slower migrated band was shifted and corresponded to the faster migrated band as a result of the λ phosphatase treatment. Therefore, the slower migrated and the faster migrated bands are phosphorylated and dephosphorylated forms of HIF-1 α , respectively. These results demonstrated that the phosphorylation status of HIF-1 α changed during hypoxia-induced apoptosis.

Expression of ARNT also changed during the prolonged hypoxia. As shown in Figure 2a, 95 kDa of ARNT protein decreased, and instead, an additional smaller band (~75 kDa) appeared. The appearance of the 75-kDa ARNT was coincidental to activation of caspase-9, as determined by production of the 35-kDa active fragment (Figure 2a). The caspase-9 activation was preceded by induction of p53- and Bax-expression, translocation of Bax to mitochondria and release of cytochrome *c* (Figure 2b,c), indicating that prolonged hypoxia activated the p53-dependent apoptotic pathway in MCF-7 cells. The caspase inhibitor Z-Asp inhibited the cleavage of ARNT as well as induction of apoptosis (Figure 2d). The same induction of HIF-1 α dephosphorylation, p53 expression and ARNT cleavage were also observed in human ovarian cancer A2780 cells, which have wild-type p53 (Figure 2e).

A



B



C

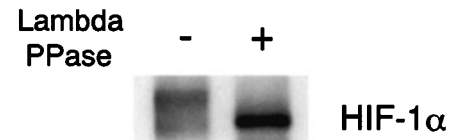


Figure 1 Induction of apoptosis by hypoxia in breast carcinoma MCF-7 cells. Cells were treated with hypoxia for the indicated times. (a) Cell viability was determined by Trypan blue dye exclusion. Bars are means \pm s.d. of triplicate determinations. (b) Total cell lysates were assayed by immunoblotting using an anti-HIF-1 α antibody. (c) Cells were treated with hypoxia for 48 h. Cell lysates were immunoprecipitated using anti-HIF-1 α antibody. The immunoprecipitates were then treated with or without λ phosphatase and resolved in SDS-PAGE. Immunoblot analysis was performed using an antibody against HIF-1 α

Caspase-mediated cleavage of ARNT

To investigate whether ARNT protein was directly cleaved by caspases, we incubated *in vitro* translated ARNT with recombinant active caspases-3 and -9. The ARNT protein was cleaved by both caspases-3 and -9, resulting in production of the 75-kDa fragment of ARNT, as observed in the above-mentioned apoptotic cells (Figure 3b, lanes 1–3). ARNT mutant proteins such as D151A and D161A, in which the aspartic acid codon was converted to alanine codon, were incubated

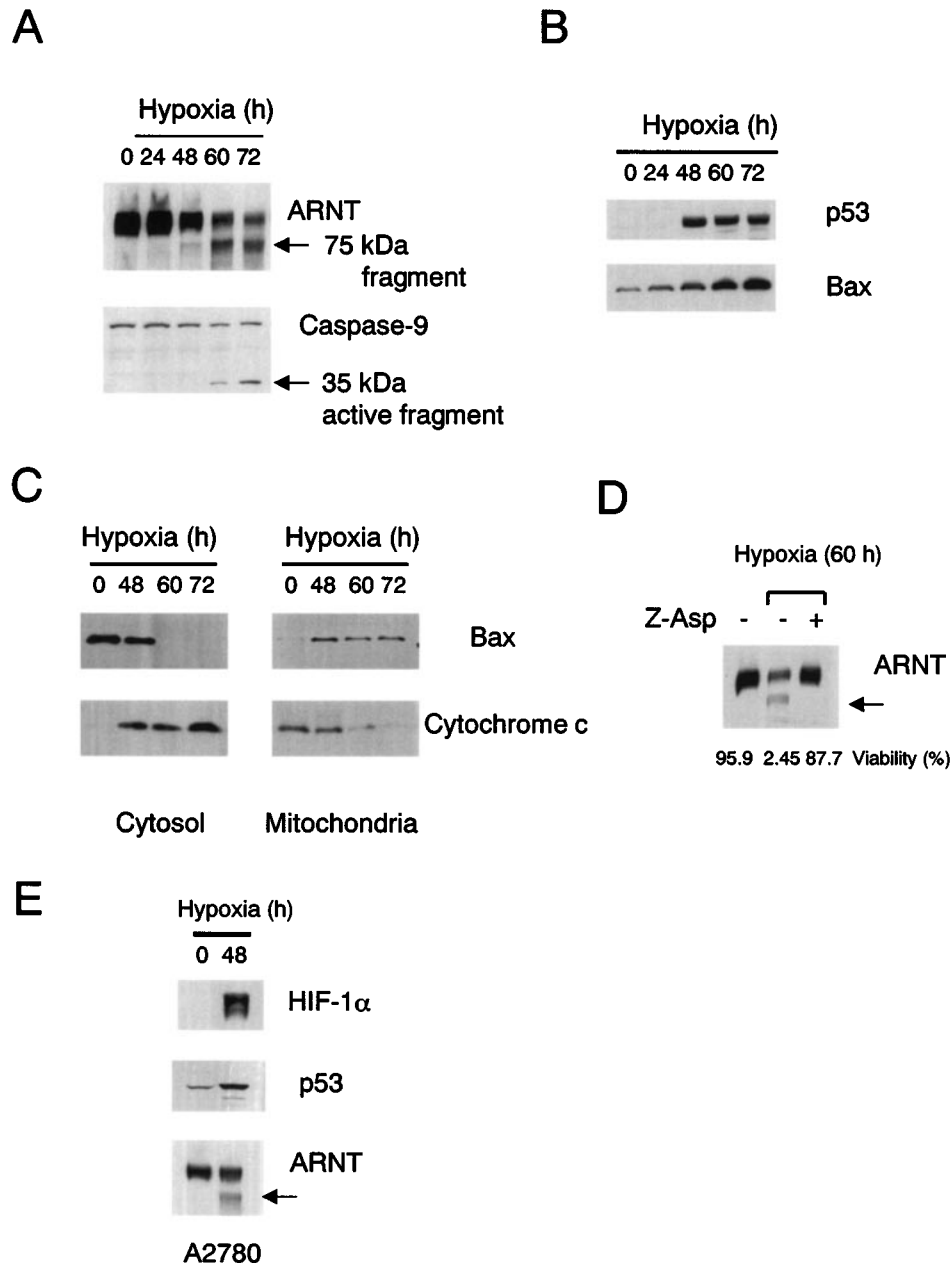


Figure 2 Cleavage of ARNT during hypoxia-induced apoptosis. (a) MCF-7 cells were treated with hypoxia for the indicated times. Total cell lysates were assayed by immunoblotting using antibodies against ARNT and caspase-9. (b) Total cell lysates were assayed by immunoblotting using antibodies against p53 and Bax. (c) Cytosolic and mitochondrial fractions were prepared and assayed by immunoblotting using antibodies against Bax and cytochrome *c*. (d) Caspase inhibitor Z-Asp inhibited the cleavage of ARNT and apoptosis. Cells were treated with hypoxia for 60 h with or without Z-Asp-CH2-DCB (100 μ g/ml). Total cell lysates were assayed by immunoblotting using anti-ARNT antibody. Cell viability was determined by Trypan blue dye exclusion. (e) A2780 cells were treated with hypoxia for 48 h. Total cell lysates were assayed by immunoblotting using antibodies against HIF-1 α , p53 and ARNT

with recombinant caspase-3. We found that the D151A ARNT was not cleaved, but other mutant proteins were cleaved by caspase-3 (Figure 3a, lanes 4–8). The D151A ARNT was also resistant to cleavage by caspase-9 (Figure 3b, lane 6). However, the D219A protein, despite mutation at DDVD²¹⁹, which is consistent with the conserved sequence (DXXD) recognized by caspase-3, was cleaved by both caspases-3 and -9 (Figure 3b, lanes 7–9).

To confirm the caspase-mediated cleavage of ARNT *in vivo*, we transfected C-terminal V5-tagged wild-type (WT) or D151A ARNT into HT1080 cells. When the transfected cells were exposed to hypoxia, the 75-kDa fragment of the WT-ARNT was produced with apoptosis induction (Figure 3c). The level of the 75-kDa fragment of D151A ARNT was lower than that of the WT-ARNT (Figure 3c). The Asp¹⁵¹ is located between the bHLH and PAS domain of ARNT protein

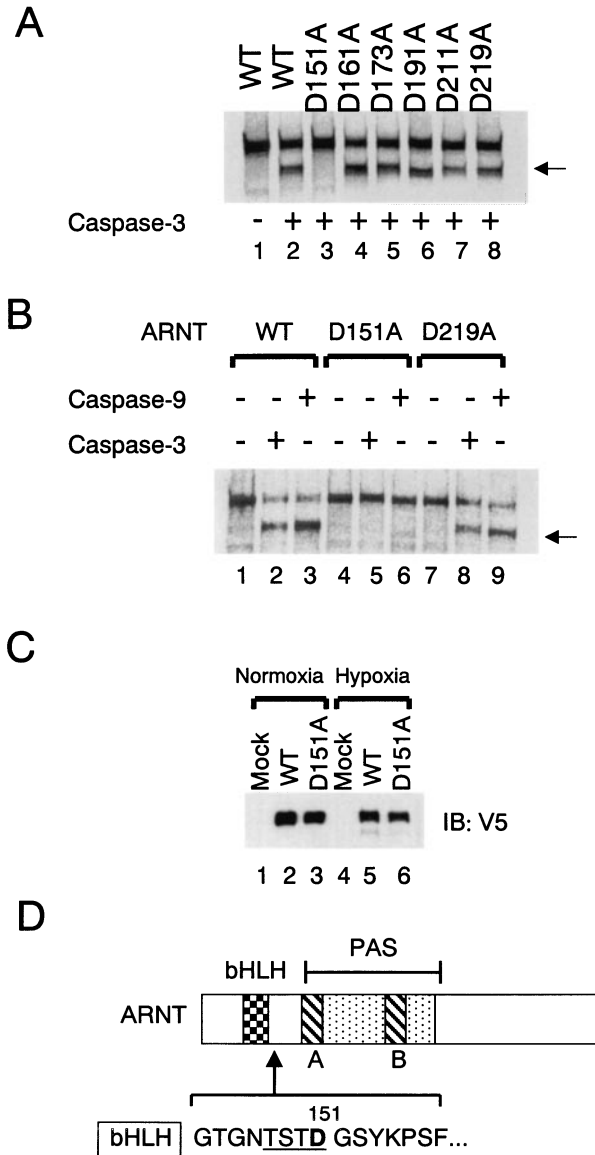


Figure 3 Identification of ARNT cleavage site by caspases-3 and -9 (a) ^{35}S -labeled ARNT wild-type (WT) and alanine-substituted mutant proteins were treated with recombinant caspase-3. The reaction mixtures were resolved in SDS-PAGE, followed by autoradiography. (b) ^{35}S -labeled ARNT wild-type (WT) and D151A, D219A mutant proteins were treated with recombinant caspases-3 and -9. (c) HT1080 cells were transfected with C-terminal V5-tagged WT ARNT and D151A ARNT mutant. After transfection, cells were treated with hypoxia for 20 h. Total cell lysates were assayed by immunoblotting using anti-V5 antibody. (d) ARNT was cleaved between bHLH and PAS domain. Amino acid sequence of ARNT after bHLH domain was described. Underline indicates the cleaved site recognized by caspases-3 and -9. (A) and (B) indicate the repeated sequences within the PAS domain

(Figure 3d), and therefore the 75-kDa fragment of ARNT would lose the bHLH domain.

ARNT-dependent phosphorylation of HIF-1 α

To investigate the relationship between the cleavage of ARNT and the phosphorylation status of HIF-1 α , we

transfected FLAG-tagged WT-ARNT or ΔN -ARNT (a.a 152–789) with V5-tagged HIF-1 α into MCF-7 cells. Subsequently, the cell lysates were immunoprecipitated with anti-FLAG antibody. In this experiment system, we could detect the binding of HIF-1 α with WT-ARNT under normoxic conditions. In contrast, HIF-1 α binding with ΔN -ARNT was not detected (Figure 4a, upper panel), although the expression levels of WT- and ΔN -ARNT were comparable (Figure 4a, middle panel). These results were consistent with the fact that bHLH domain is essential for heterodimerization among the bHLH-PAS proteins (Semenza, 2000). In the experiment, we observed that HIF-1 α in cells co-transfected with WT-ARNT mobilized as a higher molecular weight protein, than cells transfected with HIF-1 α alone or HIF-1 α and ΔN -ARNT (Figure 4a, lower panel). Treatment of the immunoprecipitated HIF-1 α from each cell lysate with λ phosphatase produced the same fast migrated, dephosphorylated form of HIF-1 α (Figure 4b). These results indicated that WT-ARNT, but not ΔN -ARNT, binds to HIF-1 α and that the binding results in the hyperphosphorylation of HIF-1 α .

We next examined the relationship between ARNT binding and the phosphorylation status of endogenous HIF-1 α . For this purpose, MCF-7 cells were exposed to hypoxia for 48 h because under the conditions, the amounts of phosphorylated and dephosphorylated HIF-1 α were nearly equal. The cell lysates were divided into two aliquots and were immunoprecipitated with either the anti-ARNT antibody or the anti-HIF-1 α antibody, followed by immunoblot analysis with the anti-HIF-1 α antibody. As shown in Figure 4c, phosphorylated HIF-1 α was preferentially co-immunoprecipitated with ARNT. The ratio of the phosphorylated to the dephosphorylated form of HIF-1 α was 4.6, when immunoprecipitation was performed using the anti-ARNT antibody. In the case of immunoprecipitation with the anti-HIF-1 α antibody, the ratio was 1.3. Thus, HIF-1 α bound to ARNT was mainly the phosphorylated form.

The role of dephosphorylated HIF-1 α in hypoxia-induced apoptosis

To examine the binding between HIF-1 α and p53, MCF-7 cells were exposed to hypoxia for 48 h, and the cell lysates were immunoprecipitated with an anti-p53 antibody. As shown in Figure 5, the dephosphorylated form of HIF-1 α was preferentially immunoprecipitated by the anti-p53 antibody. Thus, HIF-1 α bound to both ARNT (as above) and p53 under hypoxic conditions, but the phosphorylation status of HIF-1 α was different.

We next screened compounds to affect the expression of HIF-1 α in hypoxia and found that herbimycin A (HA), a tyrosine kinase inhibitor, inhibited the induction of dephosphorylated HIF-1 α (Figure 6a). Geldanamycin A (GA) also inhibited the hypoxic induction of dephosphorylated HIF-1 α . Induction of p53 was also suppressed by HA and GA (Figure 6a). GA showed the same dose dependency with respect to

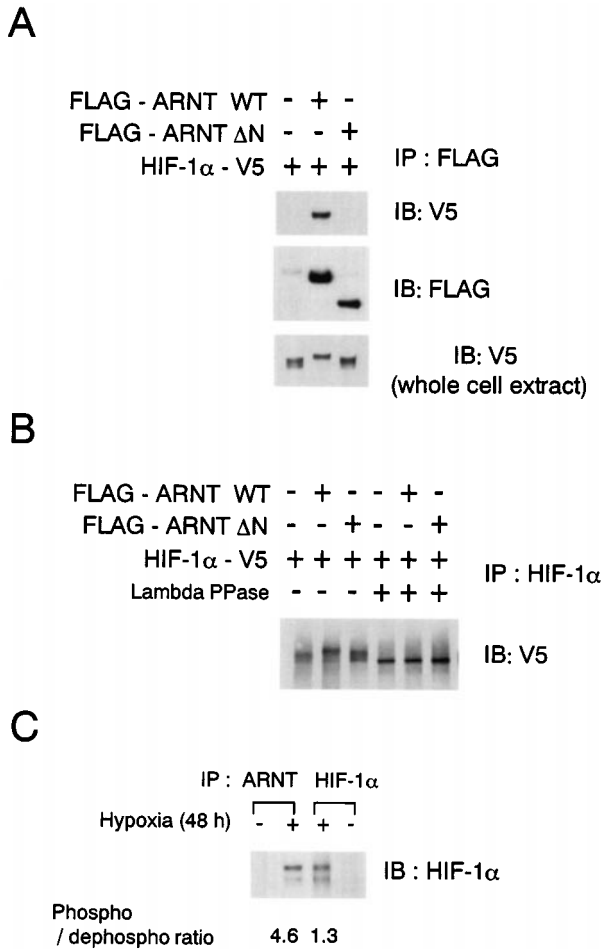


Figure 4 bHLH-truncated ARNT (Δ N) did not bind to HIF-1 α , nor induce the binding-mediated phosphorylation of HIF-1 α . MCF-7 cells were transiently transfected with FLAG-tagged wild-type WT-ARNT, bHLH truncated ARNT (Δ N) and V5-tagged HIF-1 α , as indicated. (a) Cell lysates were immunoprecipitated using anti-FLAG affinity gel, and the immunoprecipitates were resolved in SDS-PAGE. Immunoblot analysis was performed using anti-V5 (upper panel) and FLAG (middle panel) antibodies. Total cell lysates were assayed by immunoblotting using the anti-V5 antibody (lower panel). (b) Cell lysates were immunoprecipitated using anti-HIF-1 α antibody. Immunoprecipitates were treated with λ phosphatase and resolved in SDS-PAGE. Immunoblot analysis was performed using anti-V5 antibody. (c) Cells were treated with hypoxia for 48 h. Cell lysates were immunoprecipitated using antibodies against ARNT and HIF-1 α . The immunoprecipitates were then resolved in SDS-PAGE. Immunoblot analysis was performed using HIF-1 α antibody

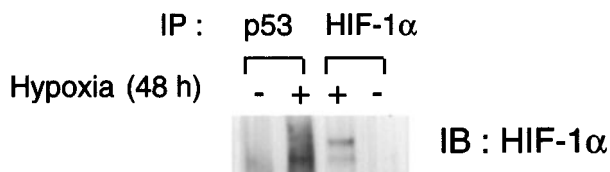


Figure 5 Interaction between HIF-1 α and p53. Cells were treated with hypoxia for 48 h. Cell lysates were immunoprecipitated using anti-p53 (DO-1) and HIF-1 α antibody. The immunoprecipitates were then resolved in SDS-PAGE. Immunoblot analysis was performed using HIF-1 α antibody

the inhibition of HIF-1 α dephosphorylation and the inhibition of p53 expression (Figure 6b). However, GA did not affect the binding between the phosphorylated HIF-1 α and ARNT (Figure 6d). HA and GA are benzoquinone ansamycins and are known to bind to Hsp90 and to interfere with its chaperon activity (Grenert *et al.*, 1997). Therefore, the effects of GA and HA could be associated with inhibition of Hsp90 function but not with inhibition of tyrosine kinases. In support of this, another tyrosine kinase inhibitor, genistein, did not inhibit the induction of dephosphorylated HIF-1 α or expression of p53 (Figure 6a, lane 5). Inconsistent with inhibition of p53 induction, GA and HA inhibited induction of Bax and blocked hypoxia-induced apoptosis (Figure 6a,c).

Interestingly, GA did not inhibit the induction of p53 by DNA-damaging antitumor agents, including mitomycin C, camptothecin and adriamycin (Figure 6e, middle panel). Thus, the mechanism of p53 stabilization under hypoxia is different from that induced by DNA damage. In agreement, hypoxia did not induce the phosphorylation of p53 (Ser-15) (Figure 6e, lower panel). The Ser-15 phosphorylation is known to stabilize p53 upon DNA damage (Shieh *et al.*, 1997), and the phosphorylation of p53 was indeed induced by the DNA damaging agents (Figure 6e, lower panel). Meanwhile, these DNA damaging agents did not induce HIF-1 α (Figure 6e, upper panel), indicating that stabilization of p53 *per se* does not cause induction of HIF-1 α .

Inhibition of nuclear accumulation of HDM2 by GA

HDM2 plays a central role in p53 degradation under normal conditions. Under normoxic conditions, HDM2 localized in the cytoplasm rather than in the nucleus (Figure 7a,b). The majority (98%) of the cells showed this cytoplasmic localization of HDM2. Under hypoxic conditions, however, HDM2 localized in the nucleus in most (97%) cells (Figure 7a,b). Interestingly, GA, which suppressed induction of p53, as above, reduced hypoxia-induced nuclear accumulation of HDM2 (Figure 7a,b). The changes in HDM2 localization were confirmed by biochemical fractionation analysis (Figure 7c). In contrast to the localization, total expression of HDM2 was hardly affected by hypoxia, in the presence or absence of GA (Figure 7c, lower panel). These results demonstrate that the nuclear localization of HDM2 correlates well with p53 stabilization under hypoxia.

Discussion

The hypoxic induction of p53 and subsequent apoptosis induction occur at 0.02% but not at 0.2% O₂ in mouse embryonic fibroblasts (Graeber *et al.*, 1996). Thus, apoptosis induction depends on the severity of the hypoxia. An *et al.* (1998) demonstrated that the induction of p53 under severe hypoxia is HIF-1 α dependent and may be achieved as a result of the

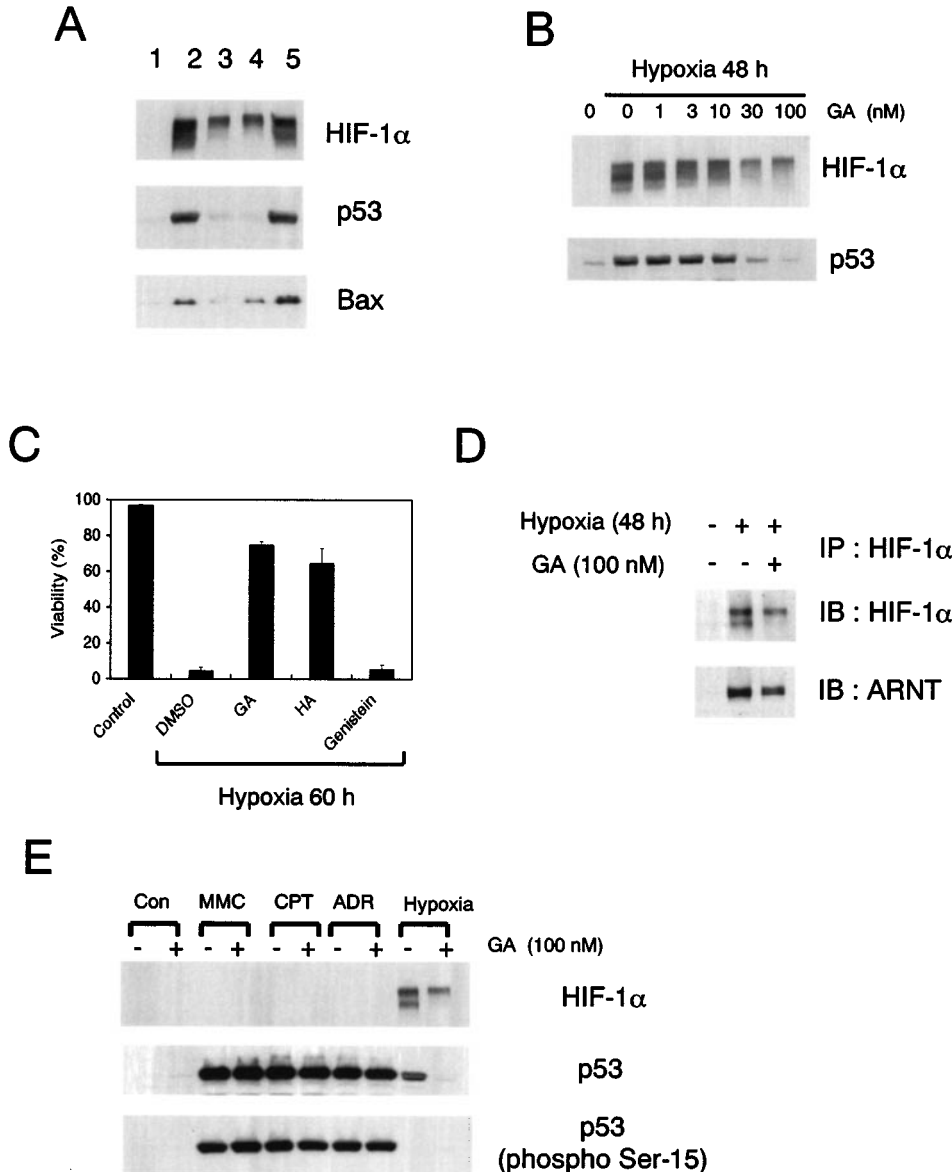


Figure 6 Geldanamycin A and herbimycin A inhibit hypoxia-induced p53 expression and HIF-1 α dephosphorylation. (a) MCF-7 cells were left untreated (lane 1) or treated with hypoxia for 48 h in the absence (lane 2) or the presence of 100 nM geldanamycin A (GA) (lane 3), 10 μ M herbimycin A (HA) (lane 4) and 10 μ M genistein (lane 5). Total cell lysates were assayed by immunoblotting using antibodies against p53, HIF-1 α and Bax. (b) Cells were treated with hypoxia for 48 h in the absence or the presence of GA at the indicated concentrations. Total cell lysates were assayed by immunoblotting using antibodies against p53 and HIF-1 α . (c) At 60 h, cell viability was determined by Trypan blue dye exclusion. Bars are means \pm s.d. of triplicate determinations. (d) Interaction between HIF-1 α and ARNT. MCF-7 cells were treated with hypoxia for 48 h with or without 100 nM GA. Cell lysates were immunoprecipitated using anti-HIF-1 α antibody. The immunoprecipitates were then resolved in SDS-PAGE. Immunoblot analysis was performed using antibodies against HIF-1 α and ARNT. (e) Cells were treated with 10 μ g/ml of mitomycin C (MMC), 2 μ g/ml of camptothecin (CPT), 2 μ g/ml of adriamycin (ADR) for 20 h. The hypoxic treatment was for 48 h in the presence or absence of 100 nM GA. Total cell lysates were assayed by immunoblotting using antibodies against HIF-1 α , p53 and p53 (phospho Ser-15)

p53 stabilization by its association with HIF-1 α . In this study, we found that severe, prolonged hypoxia induced two major forms of HIF-1 α : dephosphorylated and phosphorylated HIF-1 α . The appearance of dephosphorylated HIF-1 α correlated well with p53 induction. We showed here that the dephosphorylated HIF-1 α was the major form that bound to p53. Furthermore, the Hsp90 inhibitor GA selectively suppressed the emergence of dephosphorylated HIF-

1 α , resulting in inhibition of p53 induction as well as apoptosis. These results collectively indicate that the dephosphorylated HIF-1 α , but not the phosphorylated form, plays a pivotal role in the stabilization of p53 and subsequent activation of the p53-dependent apoptotic pathway during severe hypoxia.

HIF-1 α , p53 and HDM2 were recently shown to form a ternary complex in response to moderate hypoxia (\sim 1% O₂) (Ravi *et al.*, 2000). In fact, HIF-

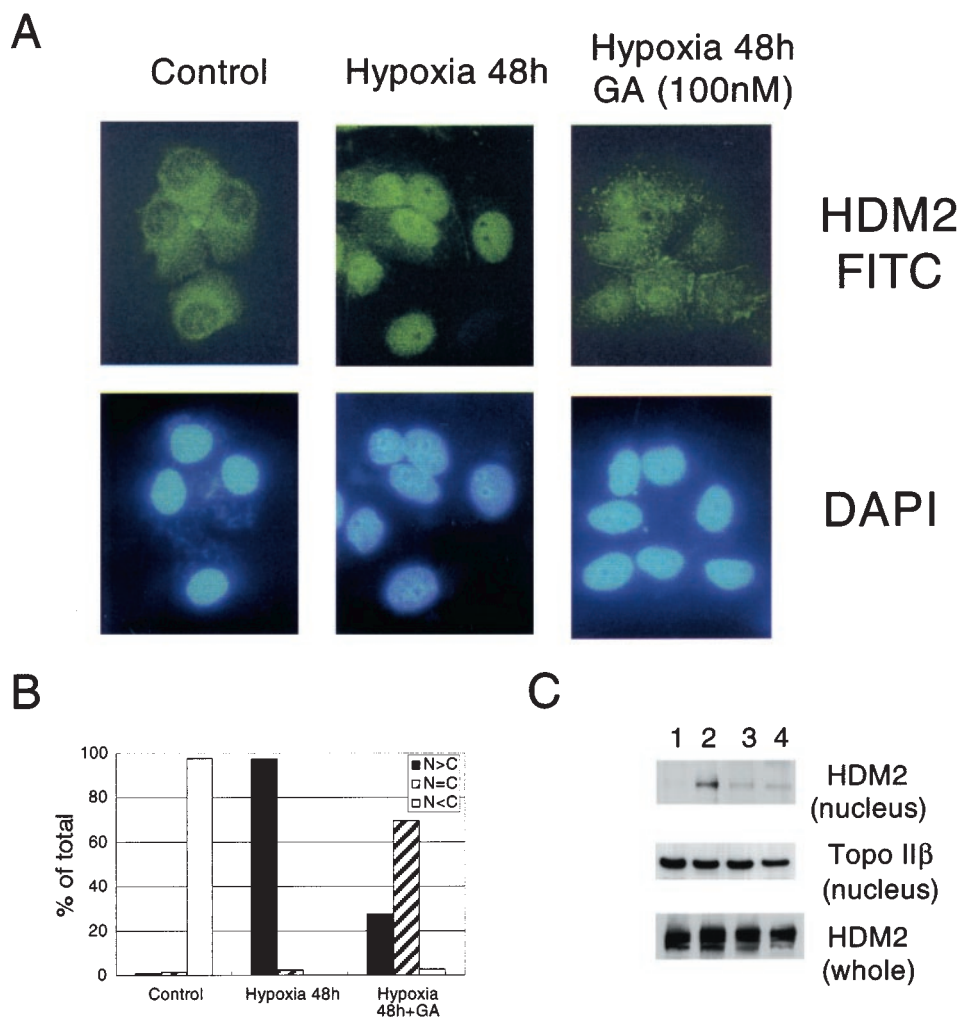


Figure 7 Geldanamycin A inhibited the nuclear accumulation of HDM2 induced by hypoxia. MCF-7 cells were treated with hypoxia for 48 h with or without 100 nM geldanamycin A (GA). (a) Localization of HDM2 was assessed using anti-HDM2 antibody and visualized using FITC-conjugated secondary antibody. Cells were counterstained with DAPI to localize the nucleus. (b) Quantification of fluorescence data from (a). Cells were scored as having fluorescence that was stronger in the nucleus (N>C), equal in the nucleus and the cytoplasm (N=C), or stronger in the cytoplasm (N<C). (c) Nuclear extract (upper and middle panel) and total cell lysates (lower panel) were assayed by immunoblotting using antibodies against HDM2 and topoisomerase II beta (Topo II β) antibody. Lane 1, control; lane 2, hypoxia 48 h; lane 3, hypoxia 48 h plus 100 nM GA; lane 4, 100 nM GA for 48 h

1 α can be induced at much higher concentrations of O₂ (~1%) than that used in this study, and the optimal O₂ concentration for HIF-1 α induction is reported to be at 0.5% (Wenger and Gassmann, 1997). However, such moderate hypoxia induces neither p53 stabilization nor p53-dependent gene expression (Wenger *et al.*, 1998). In such a situation, p53 was shown to promote HDM2-mediated ubiquitination and proteosomal degradation of HIF-1 α (Ravi *et al.*, 2000). It is likely, therefore, that the dephosphorylated HIF-1 α as well as p53 is resistant to the HDM2-mediated degradation, when they form the complex under severe hypoxic conditions. In this regard, we demonstrated that the stabilization of the dephosphorylated HIF-1 α -p53 complex was closely associated with nuclear accumulation of HDM2 (Figure 7). Several studies have shown that the nuclear-cytosolic shuttling of HDM2, together with the nuclear export of p53, is important for p53

degradation under normoxic conditions (Boyd *et al.*, 2000; Geyer *et al.*, 2000; Roth *et al.*, 1998). Indeed, inhibition of nuclear export by leptomycin B was shown to induce both p53 stabilization and HDM2 accumulation in the nucleus (Freedman and Levine, 1998; Geyer *et al.*, 2000). Thus, our observations indicate that the complex between dephosphorylated HIF-1 α and p53 may stabilize through the nuclear localization of p53 and HDM2 under severe hypoxic conditions.

Our present findings indicate that a GA-inhibitable step exists upstream of the dephosphorylated HIF-1 α -p53 complex formation. GA can inhibit the molecular chaperon Hsp90, which regulates and stabilizes many client proteins (for review see Mayer and Bukau, 1999; Scheibel and Buchner, 1998). In fact, Hsp90 was shown to bind to HIF-1 α (Gradin *et al.*, 1996), raising the possibility that the stability of dephosphorylated HIF-

1 α might be regulated by Hsp90. Alternatively, it is also possible that GA might inhibit the mitochondria-resident Hsp90 family protein, TRAP-1 (Felts *et al.*, 2000), and the endoplasmic reticulum-resident GRP94 (Chavany *et al.*, 1996). In support of this idea, these organelles have been shown to play critical roles in responding to hypoxia (Chandel *et al.*, 1998; Kaufman, 1999). Thus, further studies are needed to elucidate the mechanisms of the action of GA in the apoptotic pathway that is activated by severe hypoxia.

In contrast to p53, ARNT bound preferentially to the phosphorylated form of HIF-1 α . We also presented evidence that ARNT binding stimulates phosphorylation of HIF-1 α . These are consistent with previous observations that the heterodimerization of ARNT and HIF-1 α and the phosphorylation of HIF-1 α are required for the transcription activity of the HIF-1 complex (Richard *et al.*, 1999; Semenza, 2000). Meanwhile, the ARNT protein was subjected to the caspase-mediated cleavage during apoptosis. We identified the TSTD¹⁵¹ sequence between the bHLH and PAS domains as a cleavage site that is recognized by caspases-3 and -9 *in vitro*. Because MCF-7 cells lack caspase-3 (Janicke *et al.*, 1998), caspase-9 is likely responsible for the ARNT cleavage in the cells, although we cannot rule out the possibility of involvement of other caspases. More important, the cleavage of ARNT results in the loss of the bHLH domain, which is essential for heterodimerization with HIF-1 α and DNA binding, and ultimately for HIF-1 transcription activity (Semenza, 2000). Another important consequence of the loss of the bHLH domain is that the truncated ARNT loses the ability to stimulate the binding-dependent phosphorylation of HIF-1 α . Thus, the caspase-mediated ARNT cleavage may provide an explanation for the decrease in phosphorylated HIF-1 α with apoptosis progression.

Based on these observations, we propose the model shown in Figure 8. When O₂ concentration is reduced, HIF-1 α stabilizes and binds to ARNT. The heterodimerization stimulates phosphorylation of HIF-1 α , resulting in the formation of active HIF-1 that transactivates various genes required for improving the microenvironment, such as the angiogenic factor VEGF, and also genes for adapting to the hypoxic conditions, such as glycolytic enzymes. However, when hypoxia is severe and prolonged, the dephosphorylated form of HIF-1 α emerges and leads to p53 stabilization, which induces the Bax-mediated release of cytochrome *c* from mitochondria and the activation of caspases. The activated caspases, in turn, cleave ARNT and turn off the HIF-1-mediated transcription. In addition, the caspase-mediated cleavage of ARNT accelerates apoptosis through an increase in the dephosphorylated HIF-1 α . Thus, the dephosphorylated HIF-1 α may act as a molecular switch that activates the p53-dependent apoptotic pathway under severe hypoxic conditions.

Recently, the diminished apoptotic and the enhanced angiogenic potential of cancer cells have been recognized as key factors for development of solid

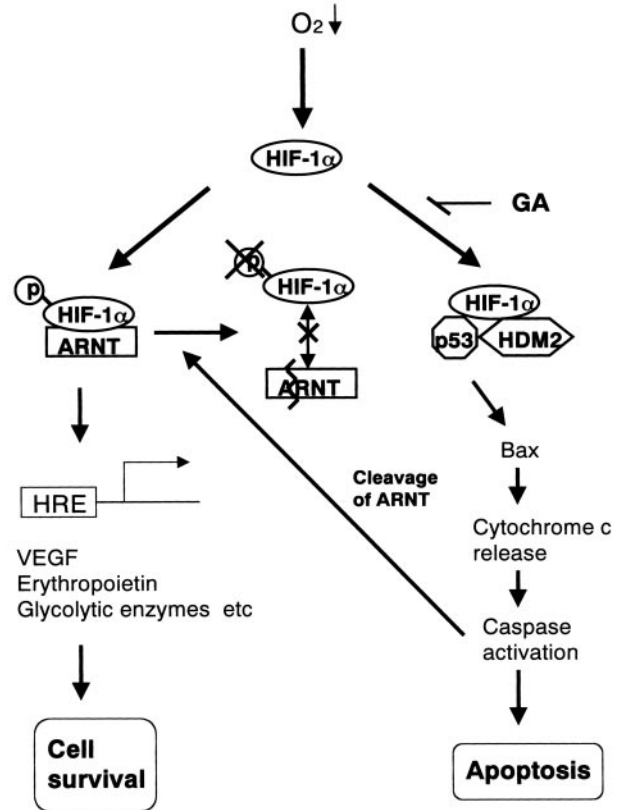


Figure 8 A proposed model of HIF-1 α function in response to hypoxia

tumors, which generally have hypoxic regions (Helminger *et al.*, 1997; Vaupel, 1997). The tumor hypoxia is thought to act as physiological pressure for the expansion of variants that have such phenotypes (Graeber *et al.*, 1996). As p53 mediates hypoxia-induced apoptosis (Graeber *et al.*, 1996) and inhibits HIF-1 activity (Blagosklonny *et al.*, 1998), inactivation of p53 can be a principal mechanism for conferring apoptosis resistance with an enhanced angiogenic phenotype. Indeed, the p53 tumor suppressor gene is frequently mutated, and p53 mutations occur in ~50% of all human cancers (Levine, 1997). However, there are many solid tumor cell lines that express wild-type p53, such as the breast carcinoma MCF-7 used in this study. These p53-expressing solid tumor cells would have also acquired an apoptosis-resistant phenotype during advanced tumor development. Indeed, we showed in this study that apoptosis induction of MCF-7 cells requires more than 48 h of exposure to hypoxic conditions, while p53-expressing mouse embryonic fibroblasts, which were oncogenetically transformed but were not selected by hypoxia, reportedly undergo apoptosis within 24 h (Graeber *et al.*, 1996). By analogy with p53, therefore, a diminished potential of HIF-1 α dephosphorylation might provide a novel mechanism for development of solid tumors that express wild-type p53 via the increase in phosphorylated HIF-1 α .

Materials and methods

Materials and antibodies

Geldanamycin A and adriamycin were obtained from Sigma (St Louis, MO, USA). Herbimycin A and genistein were from WAKO (Osaka, Japan). Z-Asp-CH2-DCB was from Funakoshi (Tokyo, Japan). Mitomycin C and camptothecin were kind gifts from Kyowa Hakkou (Tokyo, Japan) and Yakult (Tokyo, Japan). Anti-p53 antibody (clone PAb 1801, DO-1 for immunoprecipitation) and anti-caspase-9 antibody were from Calbiochem (La Jolla, CA, USA). Anti-HIF-1 α antibody was from Transduction Laboratory (Lexington, KY, USA) and NeoMarkers (clone OZ12, OZ15 for immunoprecipitation, Union City, MA, USA). Anti-ARNT antibody was from Transduction Laboratory and Alexis Biochemicals (clone 2B10 for immunoprecipitation, San Diego, CA, USA). Anti-Bax antibody was from Upstate Biotechnology (Lake Placid, NY, USA). Anti-FLAG M2 antibody and anti-FLAG affinity gels were from Sigma. Anti-Cytochrome *c* and Topoisomerase II beta antibody were from Pharmingen (San Diego, CA, USA). Anti-HDM2 (Ab-2) antibody was from Oncogene Research Products (Cambridge, MA, USA). Anti-p53 (phospho Ser-15) was from New England Biolabs (Beverly, MA, USA).

Cells and culture conditions

All cell lines were maintained in DMEM (Nissui, Tokyo, Japan) supplemented with 10% heat-inactivated fetal bovine serum and 100 μ g/ml of kanamycin and were cultured at 37°C in a humidified atmosphere of 5% CO₂ and 95% air. All experiments were performed using exponentially growing cells and were repeated at least twice. Hypoxic conditions were achieved using an anaerobic chamber and BBL GasPac Plus (Becton Dickinson, Cockeysville, MD, USA), which catalytically reduces oxygen levels to less than 10 p.p.m. within 90 min (Shimizu *et al.*, 1996).

Measurement of cell viability

Cell viability was determined by Trypan blue dye exclusion. Cells were suspended in Trypan blue and applied to a hemocytometer. Both viable and nonviable cells were counted. A minimum of 200 cells were counted for each data point.

Immunoblot analysis

For immunoblot analysis, whole cell lysates were prepared as described previously (Tomida *et al.*, 1996). In brief, cells were rinsed with ice-cold PBS and collected by scraping. The cell pellets were suspended in 1 \times SDS sample buffer (10% glycerol, 5% 2-mercaptoethanol, 2% SDS, 62.5 mM Tris-HCl, pH 6.8) and boiled for 5 min. Equal amounts of proteins were subjected to SDS-polyacrylamide gel electrophoresis (SDS-PAGE) and electroblotted onto a nitrocellulose membrane (Schleicher and Schnell, Dassel, Germany). Membranes were probed using an enhanced chemiluminescence detection system (Amersham, Tokyo).

Subcellular fractionation

Mitochondrial and cytosolic (S-100) fractions were prepared as described previously (Vander Heiden *et al.*, 1997).

For preparation of nuclear extract, cells were suspended in ice-cold nucleus buffer (150 mM NaCl, 1 mM KH₂PO₄, 5 mM

MgCl₂, 1 mM EGTA, 1 mM DTT, protease inhibitor cocktail [Sigma], 10% [vol/vol] glycerol, 0.2% Triton X-100 [pH 6.4]) for 10 min with gentle rocking. Nuclei were washed and resuspended in 1 \times SDS sample buffer and boiled for 5 min.

Immunoprecipitation

For immunoprecipitation, cells were lysed in a lysis buffer (10 mM HEPES-KOH [pH7.4], 142.5 mM KCl, 5 mM MgCl₂, 1 mM EGTA, 1 μ M MG-132 [Peptide Institute, Inc.], protease inhibitor cocktail, 0.5% NP-40) for 10 min at 4°C. Equal amounts of proteins were pre-cleared and immunoprecipitated using anti-HIF-1 α , ARNT and p53 (DO-1) antibody. Immunoprecipitates were then washed with buffer (10 mM HEPES-KOH [pH7.4], 142.5 mM KCl, 5 mM MgCl₂, 1 mM EGTA, 0.1% NP-40), resolved in SDS-PAGE, and revealed by immunoblot analysis.

Expression vector construction

Human ARNT cDNA were generated by PCR from a human testis cDNA library (Clontech, Palo Alto, CA, USA). The PCR products were cloned into a pcDNA3.1/V5-His-TOPO vector (Invitrogen, Groningen, The Netherlands), which expresses His-V5 fusion proteins at the C-terminus. Substitution of aspartic acid with alanine was accomplished using the Quick change site directed mutagenesis kit (Stratagene, La Jolla, CA, USA). All constructs were confirmed by sequencing. FLAG-tagged WT-ARNT and Δ N-ARNT (p75 fragment) were generated by inserting the corresponding ARNT cDNAs into the pCMV-2 vector (Sigma), which expresses FLAG fusion proteins at the N-terminus. Human HIF-1 α was generated by PCR from human testis cDNA library. HIF-1 α cDNA was cloned into a pcDNA3.1/V5-His-TOPO vector, which expresses V5 fusion proteins at the C-terminus.

In vitro translation and cleavage assay

Wild type, alanine-substitute ARNT mutant proteins were labeled with ³⁵S-methionine using a rabbit reticulocyte lysate system (Promega, Madison, WI, USA). The translated lysates were incubated with active recombinant caspase-3 (Pharmingen) and caspase-9 (CHEMICON, Temecula, CA, USA) in ICE buffer (20 mM HEPES-KOH (pH 7.4), 10% glycerol and 2 mM dithiothreitol) for 1 h at 37°C. The reaction was resolved in SDS-PAGE, followed by autoradiography.

Transfection

MCF-7 cells in 6-cm plates were transiently transfected with 2 μ g of each construct (HIF-1 α -V5, FLAG-ARNT WT, FLAG-ARNT Δ N) by LipofectAMINE PLUS reagent (Gibco BRL, Rockville, MD, USA). Twenty hours after transfection, cells were collected and subjected to immunoblot analysis, immunoprecipitation and dephosphorylation assay. HT1080 cells were transfected with 1 μ g of each construct (WT ARNT-V5, D151A ARNT-V5) by Fugene 6 reagent (Roche, Indianapolis, IN, USA).

Dephosphorylation assay

HIF-1 α was immunoprecipitated using anti-HIF-1 α antibody, as described. Immunoprecipitates were then washed with the phosphatase buffer supplied by the manufacture and incubated with 400 U of λ phosphatase (New England Biolabs) for 30 min at 30°C. Proteins were resolved in SDS-PAGE and revealed by immunoblot analysis.

Immunostaining

Cells were grown on glass coverslips, fixed with 4% paraformaldehyde-PBS, permeabilized with 0.5% Triton X-100-PBS and blocked with 10% heat-inactivated fetal bovine serum. To visualize the HDM2, cells were incubated with anti-HDM2 antibody and then washed in PBS before incubating with fluorescein-conjugated goat anti-rabbit IgG (Santa Cruz, Delaware Avenue, CA, USA). Cells were counterstained with DAPI (4', 6'-diamidino-2-phenylindole)

References

- An WG, Kanekal M, Simon MC, Maltepe E, Blagosklonny MV and Neckers LM. (1998). *Nature*, **392**, 405–408.
- Blagosklonny MV, An WG, Romanova LY, Trepel J, Fojo T and Neckers L. (1998). *J. Biol. Chem.*, **273**, 11995–11998.
- Boyd SD, Tsai KY and Jacks T. (2000). *Nat. Cell. Biol.*, **2**, 563–568.
- Carmeliet P, Dor Y, Herbert JM, Fukumura D, Brusselmans K, Dewerchin M, Neeman M, Bono F, Abramovitch R, Maxwell P, Koch CJ, Ratcliffe P, Moons L, Jain RK, Collen D, Keshert E and Keshet E. (1998). *Nature*, **394**, 485–490.
- Chandel NS, Maltepe E, Goldwasser E, Mathieu CE, Simon MC and Schumacker PT. (1998). *Proc. Natl. Acad. Sci. USA*, **95**, 11715–11720.
- Chavany C, Mimnaugh E, Miller P, Bitton R, Nguyen P, Trepel J, Whitesell L, Schnur R, Moyer J and Neckers L. (1996). *J. Biol. Chem.*, **271**, 4974–4977.
- Crews ST. (1998). *Genes Dev.*, **12**, 607–620.
- Deng Y and Wu X. (2000). *Proc. Natl. Acad. Sci. USA*, **97**, 12050–12055.
- Felts SJ, Owen BA, Nguyen P, Trepel J, Donner DB and Toft DO. (2000). *J. Biol. Chem.*, **275**, 3305–3312.
- Freedman DA and Levine AJ. (1998). *Mol. Cell. Biol.*, **18**, 7288–7293.
- Geyer RK, Yu ZK and Maki CG. (2000). *Nat. Cell. Biol.*, **2**, 569–573.
- Giaccia AJ and Kastan MB. (1998). *Genes Dev.*, **12**, 2973–2983.
- Gradin K, McGuire J, Wenger RH, Kvietikova I, Whitelaw ML, Toftgard R, Tora L, Gassmann M and Poellinger L. (1996). *Mol. Cell. Biol.*, **16**, 5221–5231.
- Graeber TG, Osmanian C, Jacks T, Housman DE, Koch CJ, Lowe SW and Giaccia AJ. (1996). *Nature*, **379**, 88–91.
- Green DR and Reed JC. (1998). *Science*, **281**, 1309–1312.
- Grenert JP, Sullivan WP, Fadden P, Haystead TAJ, Clark J, Mimnaugh E, Krutzsch H, Ochel HJ, Schulte TW, Sausville E, Neckers LM and Toft DO. (1997). *J. Biol. Chem.*, **272**, 23843–23850.
- Halterman MW, Miller CC and Federoff HJ. (1999). *J. Neurosci.*, **19**, 6818–6824.
- Helminger G, Yuan F, Dellian M and Jain RK. (1997). *Nat. Med.*, **3**, 177–182.
- Janicke RU, Sprengart ML, Wati MR and Porter AG. (1998). *J. Biol. Chem.*, **273**, 9357–9360.
- Kallio PJ, Wilson WJ, O'Brien S, Makino Y and Poellinger L. (1999). *J. Biol. Chem.*, **274**, 6519–6525.
- Kaufman RJ. (1999). *Genes Dev.*, **13**, 1211–1233.
- Levine AJ. (1997). *Cell*, **88**, 323–331.
- Mayer MP and Bukau B. (1999). *Curr. Biol.*, **9**, R322–R325.
- Nicholson DW. (1999). *Cell. Death Differ.*, **6**, 1028–1042.
- Ravi R, Mookerjee B, Bhujwalla ZM, Sutter CH, Artemov D, Zeng Q, Dillehay LE, Madan A, Semenza GL and Bedi A. (2000). *Genes Dev.*, **14**, 34–44.
- Richard DE, Berra E, Gothie E, Roux D and Pouyssegur J. (1999). *J. Biol. Chem.*, **274**, 32631–32637.
- Roth J, Dobbstein M, Freedman DA, Shenk T and Levine AJ. (1998). *EMBO J.*, **17**, 554–564.
- Salceda S and Caro J. (1997). *J. Biol. Chem.*, **272**, 22642–22647.
- Scheibel T and Buchner J. (1998). *Biochem. Pharmacol.*, **56**, 675–682.
- Semenza GL. (2000). *J. Appl. Physiol.*, **88**, 1474–1480.
- Shieh SY, Ikeda M, Taya Y and Prives C. (1997). *Cell*, **91**, 325–334.
- Shimizu S, Eguchi Y, Kamiike W, Itoh Y, Hasegawa J, Yamabe K, Otsuki Y, Matsuda H and Tsujimoto Y. (1996). *Cancer Res.*, **56**, 2161–2166.
- Tomida A, Suzuki H, Kim HD and Tsuruo T. (1996). *Oncogene*, **13**, 2699–2705.
- Vander Heiden MG, Chandel NS, Williamson EK, Schumacker PT and Thompson CB. (1997). *Cell*, **91**, 627–637.
- Vaupel PW. (1997). *Klin Padiatr*, **209**, 243–249.
- Vogelstein B, Lane D and Levine AJ. (2000). *Nature*, **408**, 307–310.
- Wenger RH, Camenisch G, Desbaillets I, Chilov D and Gassmann M. (1998). *Cancer Res.*, **58**, 5678–5680.
- Wenger RH and Gassmann M. (1997). *Biol. Chem.*, **378**, 609–616.

(Sigma). The coverslips were mounted on glass slides and visualized by using a fluorescence microscope.

Acknowledgments

We thank Dr Mikihiro Naito for helpful discussions. This work was supported by a special grant for Advanced Research on Cancer, a Grant-in-Aid for Cancer Research from the Ministry of Education, Science, Sports and Culture, Japan.